Available online at www.sciencedirect.com
ScienceDirect
International Journal of Heat and Fluid Flow 28 (2007) 552–560
International Journal of HEAT AND FLUID FLOW
www.elsevier.com/locate/ijhff

Flow-induced streamwise oscillation of two circular cylinders in tandem arrangement

Atsushi Okajima [a,*], Satoru Yasui [b], Takahiro Kiwata [b], Shigeo Kimura [b]

[a] *Kanazawa-Gakuin College, 10 Sue-Machi, Kanazawa 920-1392, Japan*
[b] *School of Graduate Natural Science and Technology, Kanazawa University, Kakuma-machi, Kanazawa 920-1192, Japan*

Received 5 March 2007; accepted 1 April 2007
Available online 26 June 2007

Abstract

Flow-induced streamwise oscillation of two tandem circular cylinders has been studied by means of free-oscillation testing in a wind tunnel. One cylinder was elastically supported so as to allow it to move in the streamwise direction; the other was fixed to the tunnel sidewalls. Small values of the reduced mass-damping parameter ($Cn \leqslant 1$) have been considered. When the upstream cylinder is free to oscillate, there are two excitation regions: the first for reduced velocity, Vr, in the range $1.4 \leqslant Vr \leqslant 2.5$ and cylinder gap distance to diameter ratio, s, between 0.3 and 3, is due to movement-induced excitation accompanied by symmetrical vortex shedding, while the second, for $2.7 \leqslant Vr \leqslant 3.7$ and $1.75 \leqslant s \leqslant 3$, is due to vortex excitation by alternate Karman vortex shedding. On the other hand, the response characteristics when the downstream cylinder is free to oscillate, have an excitation region due to Karman vortex shedding from the two cylinders, connected by the dead water region between them for $2 \leqslant Vr \leqslant 4$ and $0.3 \leqslant s \leqslant 0.75$, and it is followed by a second excitation region, due to symmetrical vortex shedding, that is limited to $0.75 \leqslant s \leqslant 2$. Furthermore an unstable limited cycle oscillation with large amplitude appears for $1 \leqslant s \leqslant 1.25$, by giving an initial oscillating displacement to the cylinder. When s is greater than 2.5, the downstream cylinder experiences buffeting.

Keywords: Flow-induced oscillation; Streamwise oscillation; Two circular cylinders; Tandem arrangement; Flow visualization

1. Introduction

Flow-induced oscillation of circular cylinders has been of great interest for many decades and frequently occurs in a variety of industrial settings: nuclear power plants, heat exchangers, offshore platforms and so on. If the working fluid is a liquid such as water, oil or metal sodium at high temperature, structures with extremely small mass ratios may be easily induced to oscillate in the streamwise (in-line) direction at relatively low reduced velocities. For example, flow-induced oscillation in the streamwise direction caused damage to a thermometer well and sodium leakage at "Monju", the Japan Nuclear Cycle Development Institute's prototype fast breeder reactor, in 1995 (JSME, 2001; Okajima et al., 2004a).

Vortex shedding from an elastically supported cylinder can cause the cylinder to oscillate in the cross-flow (transverse), and streamwise directions if there is little structural damping. In addition, since the value of the mass ratio M, defined by $M = m/\rho D^2$ where m is the mass per unit span length, ρ is the fluid density and D is the cylinder diameter, is small in liquid flows, the streamwise oscillation of cylinders may easily occur at low reduced velocity, because the reduced mass-damping parameter Cn ($=2M\delta$, where δ is the logarithmic decrement of the structure damping parameter) is small.

There already exist some studies on the streamwise oscillation of circular cylinders. For example, King et al. (1973) carried out experiments on a flexible cantilevered circular cylinder beam in a water channel. They reported that

* Corresponding author. Tel.: +81 76 229 8816; fax: +81 76 229 8968.
E-mail address: a-okaji@kanazawa-gu.ac.jp (A. Okajima).

0142-727X/$ - see front matter © 2007 Elsevier Inc. All rights reserved.
doi:10.1016/j.ijheatfluidflow.2007.04.015

Nomenclature

Cn	Reduced mass-damping parameter, $2M\delta$	St_w	wake Strouhal number, f_wD/U
D	cylinder diameter	s	nondimensional gap distance between the cylinders, S/D
f_c	characteristic frequency of a cylinder	U	uniform flow velocity
f_n	natural frequency for vortex shedding from stationary cylinders	Vr	reduced velocity, U/f_cD
f_w	wake frequency	Vr_{cr}	reduced resonance velocity, $U/f_nD = 1/St_n$
M	mass ratio, $m/\rho D^2$	X_{rms}	nondimensional root-mean-square response amplitude of a cylinder, x_{rms}/D
m	cylinder mass per unit span length	x_{rms}	root-mean-square response amplitude of a cylinder
Re	Reynolds number, UD/v	δ	logarithmic decrement of the structure damping parameter of a cylinder
S	gap distance between the cylinders	v	kinematic viscosity of the working fluid
St_c	nondimensional characteristic frequency of a cylinder, f_cD/U	ρ	fluid density
St_n	wake Strouhal number for a stationary cylinder, f_nD/U		

streamwise oscillation of the cylinder occurs with large amplitude when Cn is less than 1. Streamwise oscillations occur in two regions near half of the resonance velocity; the one at lower velocity is termed the first excitation region, and the one at higher velocity is termed the second excitation region (King et al., 1973). Recently, in addition to numerical simulations (Tamura and Okada, 1998; Nakamura and Okajima, 2001), a number of experimental studies have been carried out on the streamwise oscillation of structures in wind tunnels (Okajima et al., 2000) and water tunnels (Okajima et al., 2004b), in order to evaluate the critical values of the reduced mass-damping parameter for streamwise oscillations under the same conditions as the free-oscillation tests in the cross-flow direction performed by Scruton (1963).

The situation of multiple circular cylinders placed one behind the other in a flow occurs in many areas of engineering (e.g. aeronautical, hydronautical, civil, offshore) and is known to lead to flow-induced oscillations (e.g. Okajima, 1982; Laneville and Brika, 1999; Feenstra et al., 2003; Assi et al., 2006). In this work, therefore, we study the streamwise oscillation of an arrangement of two circular cylinders, by means of free-oscillation testing in a wind tunnel. First, the upstream cylinder is elastically supported so as to move in the streamwise direction, while the downstream cylinder is fixed; then, the downstream cylinder is allowed to oscillate, and the upstream cylinder is fixed. For both configurations, the gap distance between the cylinders is varied, and the response amplitudes of the oscillating cylinder and the vortex shedding frequency in the wake are measured. In addition, the smoke-wire method is used to visualize the flow around the cylinders.

The layout of this paper is as follows. Section 2 presents an outline of the experimental arrangement. In Section 3, our results are compared with previous works. Section 4 gives the response characteristics of the upstream cylinder when it is free to undergo streamwise oscillation, whilst Section 5 gives results for the case when the downstream cylinder is free to oscillate. Finally, conclusions are drawn in Section 6.

2. Experimental arrangement

Experiments were performed in a low-speed and open-type wind tunnel with a rectangular working section of 300 mm × 1200 mm, as shown in Fig. 1. Two circular cylinders, each with a diameter, D, of 120 mm and made of Styrofoam with smooth surfaces covered by aluminum foil, were used. The span length of each cylinder was 293 mm, and the blockage ratio of cylinders in a wind tunnel was 10%. Circular end plates, approximately 240 mm in diameter and 0.5 mm thick, were fixed to both sides of the oscil-

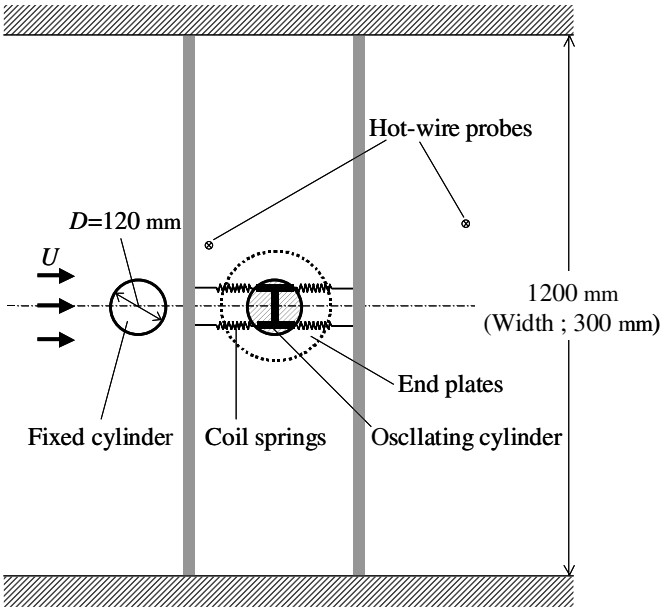

Fig. 1. Schematic view of a test section for experiment; the downstream cylinder elastically supported to move in the streamwise direction, is free to oscillate, while the upstream cylinder is fixed.

lating cylinder, so as to reduce the influence of any end-effects on the flow. The oscillating cylinder was supported by eight coil springs in order to allow it to move in the streamwise direction only. The characteristic frequency, f_c, of the oscillating cylinder was found to be 3.85 Hz; this is used in the definition of the nondimensional value of the characteristic frequency of a cylinder, $St_c = f_c D/U$, where U is the wind speed. The reduced mass-damping parameter (Scruton number) is defined by

$$\mathrm{Cn} = \frac{2m\delta}{\rho D^2} = 2M\delta \tag{1}$$

where m is the equivalent mass of the cylinder per unit span, ρ is the air density and δ is the logarithmic damping parameter of the oscillating system. The value of mass ratio, M ($=m/\rho D^2$) of a tested circular cylinder is evaluated to be about 160.

Three experimental configurations were considered. Fig. 2a shows the case where the upstream cylinder, elastically supported to move in the streamwise direction, is free to oscillate, while the downstream cylinder is fixed to the tunnel side-walls, whereas Fig. 2b shows the case where the downstream cylinder is free to oscillate, while the upstream cylinder is fixed. The cylinder gap distance to diameter ratio, $s = S/D$ where S is the gap distance between the upstream and downstream cylinders, was varied between 0.3 and 3. Fig. 2c shows an oscillating cylinder, behind which there is a splitter plate which suppresses the generation of alternate Karman vortex shedding and produces symmetrical wake flow (Bearman, 1967). The splitter plate was made of acrylic and was 0.3 m wide, 1.25 m long and 5 mm thick.

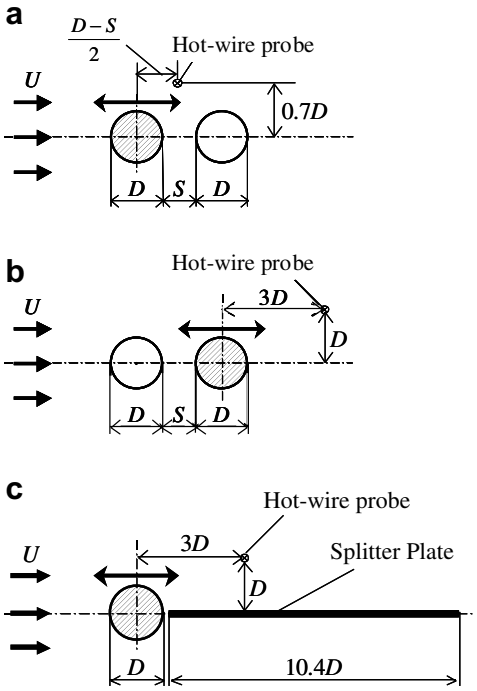

Fig. 2. Arrangement of two tandem circular cylinders and a circular cylinder with splitter plate: (a) Oscillating upstream cylinder; (b) Oscillating downstream cylinder; (c) Oscillating cylinder with splitter plate.

The response amplitude, x_{rms}, of the oscillating cylinder was measured using laser displacement detectors, and non-dimensionalized with the cylinder diameter to give the dimensionless the root-mean-square amplitude, X_{rms}. Other quantities of importance are the reduced velocity, Vr, and the wake Strouhal number, St_w, defined respectively by

$$\mathrm{Vr} = \frac{U}{f_c D} \tag{2}$$

$$St_w = \frac{f_w D}{U} \tag{3}$$

where f_w is the vortex shedding frequency, measured by hot-wire probes located on the center-line of the gap between two cylinders and in the wake, as shown in Fig. 2. In addition, the flow around the cylinders was visualized by the smoke-wire method, using liquid paraffin smoke.

3. Strouhal numbers for two stationary tandem cylinders

Fig. 3 shows the values of the Strouhal number measured in the wake behind two stationary tandem cylinders, St_w (Fig. 2b) for different values of gap distance, s, at Reynolds numbers of $Re = (1-2)\times 10^4$, in comparison with earlier results for $Re = 1.7\times 10^5$ (Okajima, 1979) and $Re = (0.15-1.5)\times 10^4$ (Ishigai et al., 1972). The present values of the Strouhal number seem to be close to those obtained at lower Reynolds numbers. It is apparent that St_w changes with s, and it is influenced by the Reynolds number at narrow gap distances less than 1. The values of St_w change from 0.14 to 0.18 near $s = 2.5$, and approach the natural frequency for vortex shedding from a single cylinder, 0.2, while St_w, obtained by the earlier works of Okajima (blockage ratio, 7.5%) and Ishigai (blockage ratio, 9.1%), has two values around $s = 2.8$. Effects of the present

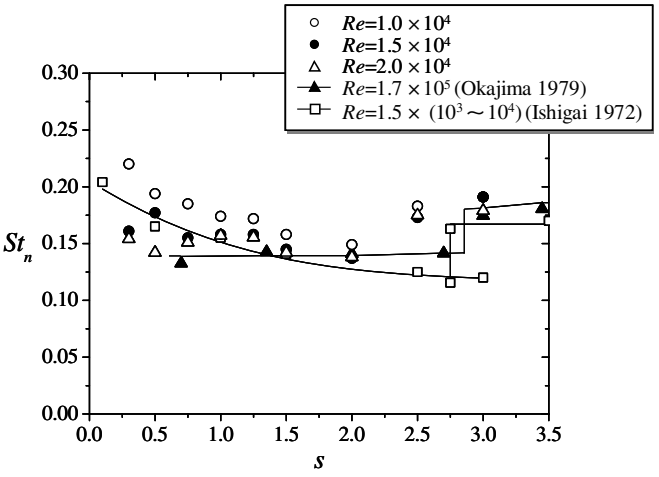

Fig. 3. Strouhal number St_n for two stationary tandem cylinders.

blockage, 10% seem to be not so large on Strouhal numbers for stationary cylinders.

4. Flow-induced streamwise oscillation of the upstream cylinder

The gap distance to diameter ratio, s, was changed from 0.3 to 3, and the flow-induced streamwise oscillation of the upstream cylinder was examined. Here, we show typical results for $s = 0.5$ (narrow gap) and 2 (wide gap).

4.1. $s = 0.5$

Fig. 4a shows an example of the response curve of the streamwise oscillation of the upstream circular cylinder for $s = 0.5$. This figure shows the nondimensional response amplitude, X_{rms}, and the wake Strouhal number, St_{w}, against reduced velocity, Vr, for the reduced mass-damping parameter $\mathrm{Cn} = 0.99$ ($\delta = 0.0031$, $M = 160$), as well as comparison with results for a single oscillating cylinder and an oscillating cylinder with a splitter plate (abbreviated to SP in Fig. 4a). In this figure, streamwise oscillations begin to occur near $\mathrm{Vr} = 1.4$, and X_{rms} increases with Vr up to a value of 0.053; oscillation-damping first occurs near $\mathrm{Vr} = 2.8$, and the cylinder ceases to oscillate completely at $\mathrm{Vr} = 3.5$. Lock-in, i.e. wake Strouhal number, St_{w}, being equal to the nondimensional characteristic frequency of a cylinder, St_{c}, is found to occur for $1.4 \leqslant \mathrm{Vr} \leqslant 3.8$.

Fig. 4b shows the visualized flow pattern when the upstream cylinder oscillates in the streamwise direction at $\mathrm{Vr} = 2.49$. In this figure, the shear layer separating from the upstream cylinder clearly rolls up into symmetrical vortices in the gap between the cylinders. It is evident that this streamwise oscillation is due to movement-induced excitation (Naudasher and Wang, 1993) accompanied by symmetrical vortices of characteristic frequency St_{c} that form in the gap.

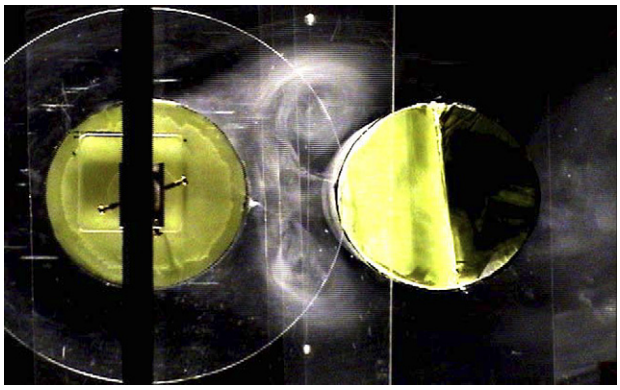

Fig. 4b. Visualized flow pattern at $\mathrm{Vr} = 2.49$ for $\mathrm{Cn} = 0.99$ and $s = 0.5$.

4.2. $s = 2$

Fig. 5a shows the results of the streamwise oscillation of the upstream cylinder for $s = 2$, i.e. when s becomes relatively large. Two excitation regions appear, one for $1.5 \leqslant \mathrm{Vr} \leqslant 2.4$ and another for $2.9 \leqslant \mathrm{Vr} \leqslant 3.6$, while X_{rms} is suppressed to a value smaller than 0.005 for $2.4 \leqslant \mathrm{Vr} \leqslant 2.9$; these response characteristics are similar to those of a single cylinder. Fig. 5a also indicates that the Strouhal frequency equals St_{c} in the first excitation region and $St_{\mathrm{c}}/2$ in the second.

Fig. 5b shows the visualized flow pattern when the upstream cylinder oscillates in the streamwise direction at $\mathrm{Vr} = 2.23$ in the first excitation region. In this figure, it is apparent that two pairs of symmetrical vortices with Strouhal number St_{c} form in the gap between the cylinders.

4.3. $0.3 \leqslant s \leqslant 1.5$

Fig. 6a summarizes the response curves of the streamwise oscillation of the upstream cylinder for values of s between 0.3 and 1.5. All curves appear to be similar to

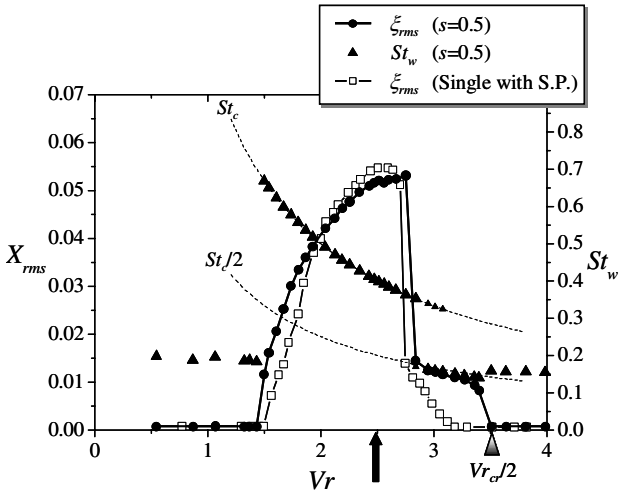

Fig. 4a. The response amplitude of the upstream cylinder and Strouhal number versus Vr.

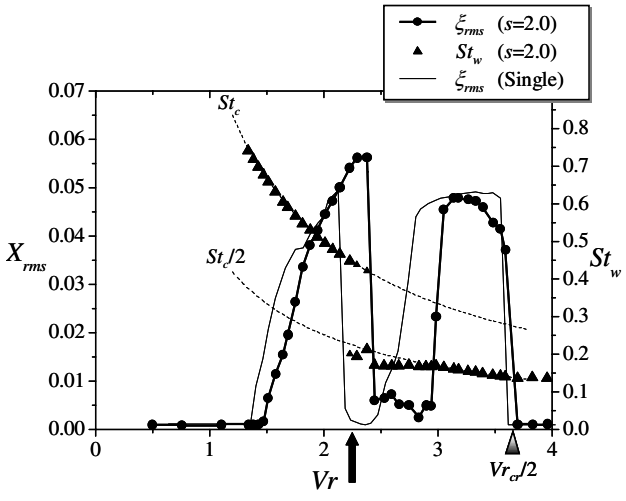

Fig. 5a. The response amplitude of the upstream cylinder and Strouhal number versus Vr.

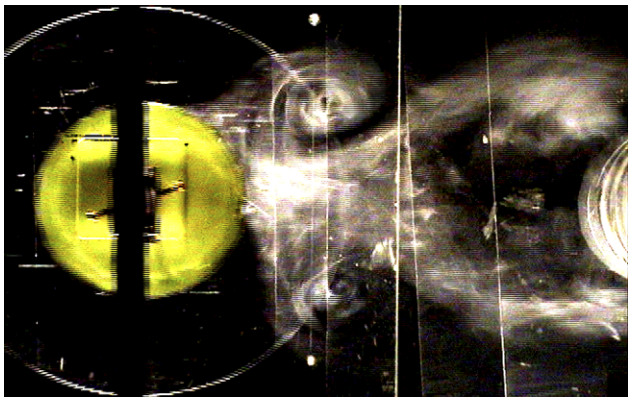

Fig. 5b. Visualized flow pattern at Vr = 2.23 for Cn = 0.99 and $s = 2$.

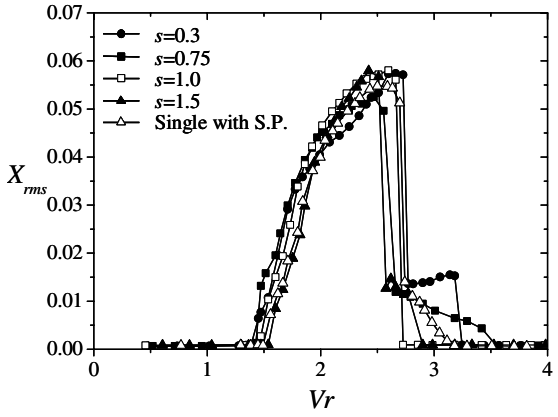

Fig. 6a. The response amplitude of the upstream cylinder in terms of Vr for Cn = 0.99 and $0.3 \leqslant s \leqslant 1.5$.

those for the response characteristics of a cylinder with a splitter plate, plotted with the symbol Δ. This implies that the downstream cylinder prevents alternate vortex shedding, in the same way as a splitter plate does. This oscillation is due to movement-induced excitation, accompanied by the formation of symmetrical vortices in the gap in front of the downstream cylinder.

4.4. $1.75 \leqslant s \leqslant 3$

The response curves for values of s between 1.75 and 3 are plotted in Fig. 6b. It is evident that all the response curves exhibit two excitation regions, and gradually approach the curve of a single cylinder when $s \geqslant 1.75$. Thus, the response characteristics of two cylinders change from one excitation region to two regions for a value of s between 1.5 and 1.75, while the value of Strouhal number for two stationary tandem cylinders, changes near $s = 2.5$, as shown in Fig. 3. The critical value of s for the response characteristics is apparently different from that of the critical value for stationary cylinders.

4.5. The excitation regions of the upstream cylinder

Fig. 7a shows the excitation regions of the upstream cylinder as functions of s and Vr. There are two kinds of exci-

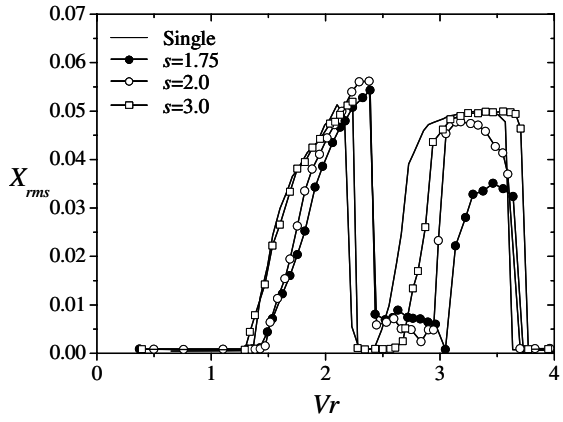

Fig. 6b. The response amplitude of the upstream cylinder in terms of Vr for Cn = 0.99 and $1.75 \leqslant s \leqslant 3$.

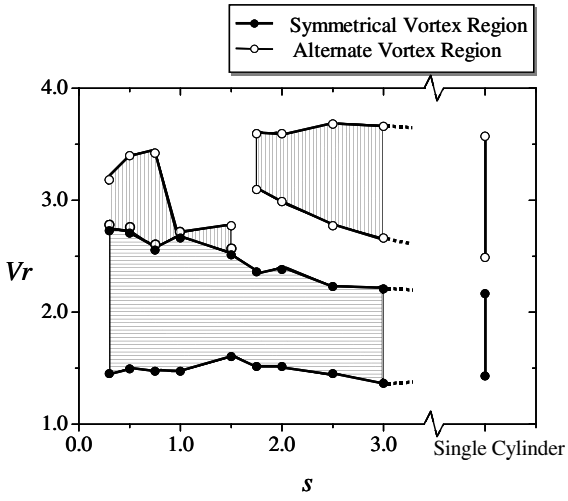

Fig. 7a. The excitation regions of the upstream cylinder as functions of s and Vr for Cn = 0.99.

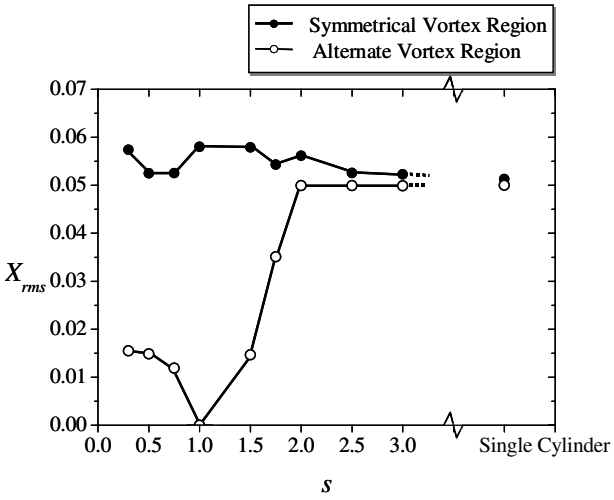

Fig. 7b. The maximum response amplitudes of the upstream cylinder in terms of s for Cn = 0.99.

tation regions, each due to different oscillation mechanisms: movement-induced excitation, accompanied by the symmetrical vortex shedding, and Karman vortex excitation. Movement-induced excitation occurs for $Vr \geqslant 1.4$ for the entire experimental range in s ($0.3 \leqslant s \leqslant 3$). For $1.75 \leqslant s \leqslant 3$, the response characteristics of the upstream cylinder have two excitation regions; these are associated with symmetrical vortex shedding and alternate Karman vortex shedding, similar to the case of a single cylinder.

Fig. 7b summarizes the maximum amplitudes of the response curves shown in Figs. 6a,6b as a function of s. For all values of s, the maximum amplitudes seem to be almost comparable to the peak value ($X_{rms} = 0.05$) for a single cylinder in the first excitation region. The maximum values of the second region at $2.7 \leqslant Vr \leqslant 3.7$ increase with s. It is evident that the oscillation of the upstream cylinder is not influenced by the presence of the downstream cylinder when s becomes greater than 2.

5. Streamwise oscillation of the downstream cylinder

Here, we show typical results for the streamwise oscillation of the downstream cylinder, when it is free to oscillate in the streamwise direction and the upstream cylinder is fixed. Results are presented for three gap distance ratios: $s = 0.5$, 1 and 2.

5.1. $s = 0.5$

Fig. 8a shows the response curve and Strouhal numbers for the downstream cylinder for $s = 0.5$ and $Cn = 0.95$ ($\delta = 0.0030$, $M = 160$), together with the results for a single oscillating cylinder. The response curve of only one excitation region with half of the characteristic frequency, $St_c/2$, is quite different from those of a single cylinder with two excitation regions; to emphasize this point, we show in Fig. 8b a visualized picture for the downstream cylinder oscillating in the streamwise direction at $Vr = 3.34$. In this

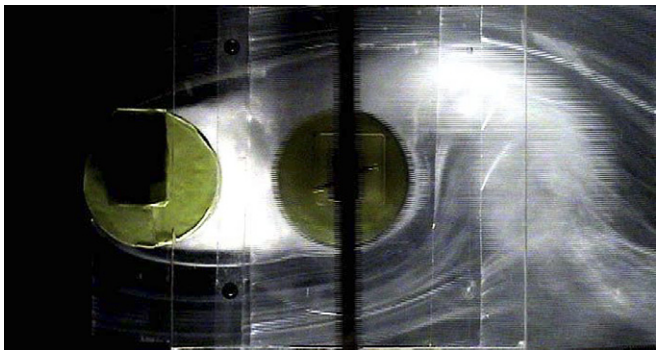

Fig. 8b. Visualized flow pattern at $Vr = 3.34$ for $Cn = 0.95$ and $s = 0.5$.

figure, the downstream cylinder oscillates with frequency $St_c/2$, locking to alternate Karman vortex shedding from the two cylinders. Here, it is as if the cylinders and the dead water region between them form a single body from which vortex shedding occurs.

5.2. $s = 1$

It is noteworthy that the response curve and Strouhal number for the downstream cylinder when $s = 1$, as shown in Fig. 9, have two excitation regions: $1.5 \leqslant Vr \leqslant 2$ and $3 \leqslant Vr \leqslant 5$. The excitation with small amplitude begins to grow at low reduced velocities; this oscillation is caused by movement-induced excitation, accompanied by symmetrical vortex shedding in the gap and also in the wake behind the downstream cylinder, as shown in Fig. 10a for $Vr = 1.71$. On the other hand, the other excitation with large amplitude in the high reduced velocity range takes the form of a so-called unstable limit cycle oscillation (Okajima, 1982); that is, when the initial oscillating displacement applied to the cylinder is greater than some critical value ($X_{rms} = 0.02$), the amplitude of oscillation increases, but is damped out otherwise. In the range

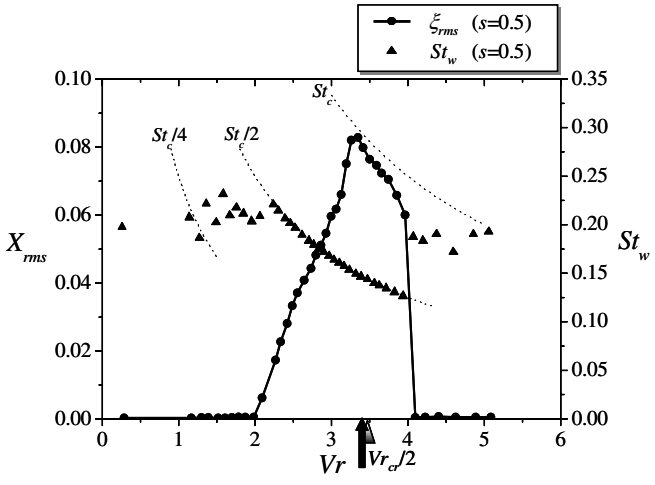

Fig. 8a. The response amplitude of the downstream cylinder and Strouhal number in terms of Vr.

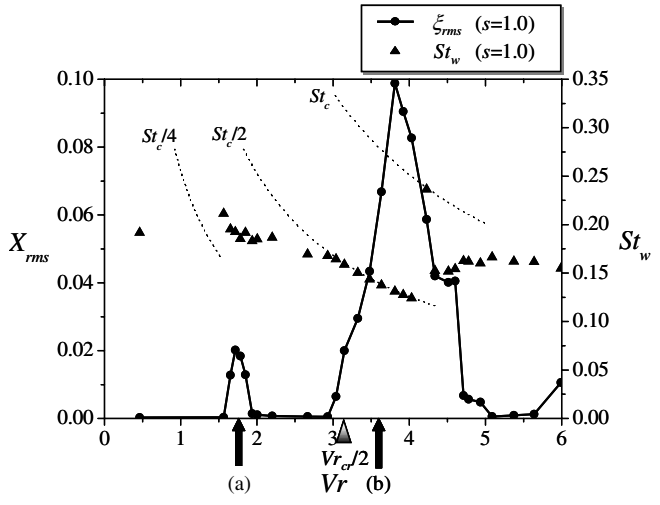

Fig. 9. The response amplitude of the downstream cylinder and Strouhal number in terms of Vr.

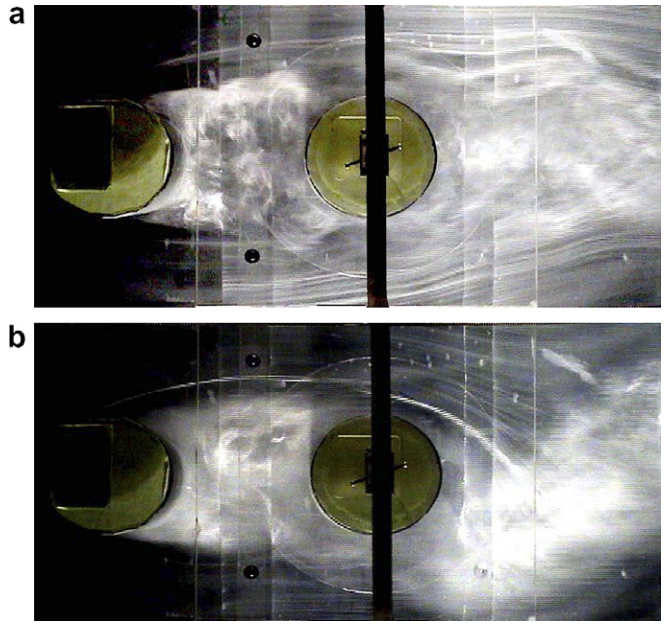

Fig. 10. Visualized flow patterns for Cn = 0.95 and $s = 1.0$ at (a) Vr = 1.71, (b) Vr = 3.56: (a) Visualized flow pattern at Vr = 1.71; (b) Visualized flow pattern at Vr = 3.56.

$3.0 < \mathrm{Vr} < 4.0$, the vortices shed in the wake lock in to half of the characteristic frequency. It is apparent from the flow pattern in Fig. 10b for Vr = 3.56 that the unstable limit cycle oscillation with large amplitude is induced by the alternate Karman vortex shedding from the two tandem cylinders, connected by the dead water region formed in the gap between them. Giving an initial oscillating displacement to the cylinder promotes the periodic reattachment of the separated shear layers of the upstream cylinder to the downstream one, which results in the unstable limit-cycle oscillation (Okajima, 1982).

5.3. $s = 2$

Fig. 11a shows the curves of the response amplitude, X_{rms}, and Strouhal number, St_{w}, when $s = 2$ and the corresponding result for a single cylinder. In this case, there is one excitation region in the reduced velocity range $2.3 \leqslant \mathrm{Vr} \leqslant 3.5$; the peak value of the amplitude ($X_{\mathrm{rms}} = 0.05$) are similar to those of a single cylinder. The visualized flow pattern for Vr = 2.64 and $s = 2$ is shown in Fig. 11b. This flow pattern is much different from the alternate Karman vortex patterns shown in Figs. 8b and 10b, and it is rather similar to the symmetrical vortex pattern of Fig. 10a. It may be concluded from the above results that this oscillation is due to movement-induced excitation, accompanied by symmetrical vortex shedding.

5.4. The excitation regions of the downstream cylinder

Fig. 12a shows the excitation regions of the downstream cylinder as a function of s and Vr. The excitation region for

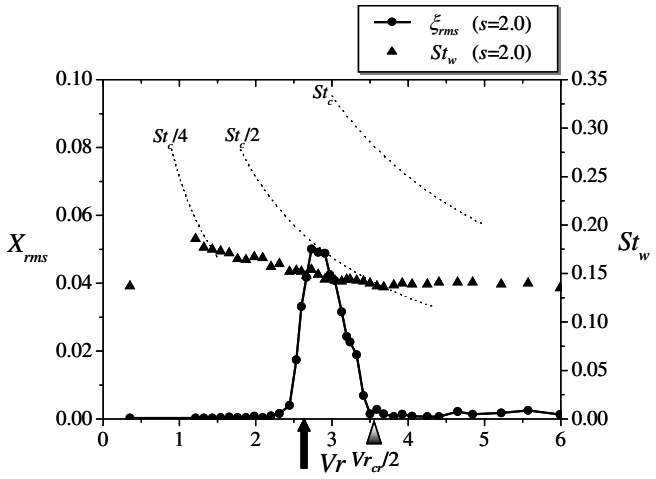

Fig. 11a. The response amplitude of the downstream cylinder and Strouhal number in terms of Vr.

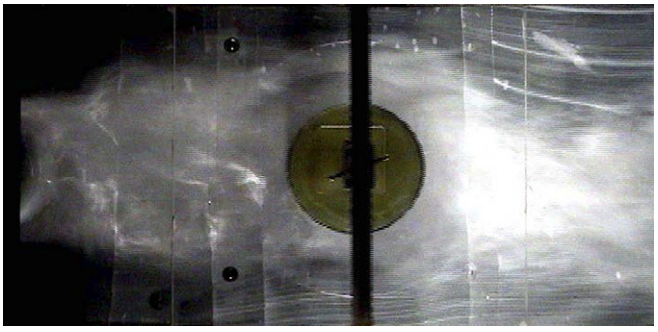

Fig. 11b. Visualized flow pattern at Vr = 2.64 for Cn = 0.95 and $s = 2.0$.

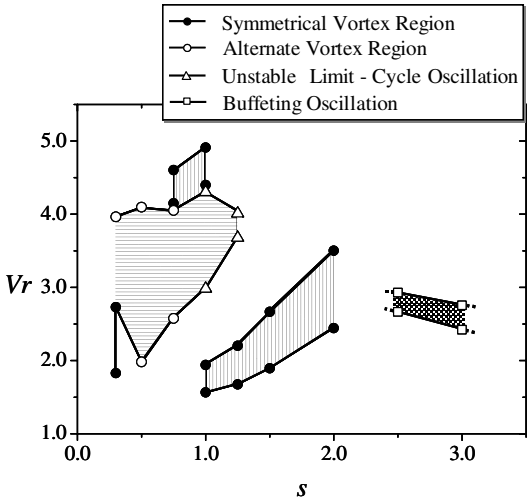

Fig. 12a. The excitation regions of the downstream cylinder as functions of s and Vr for Cn = 0.95.

$0.3 \leqslant s \leqslant 0.75$ is induced by alternate Karman vortex shedding from the two cylinders, while the excitation regions due to symmetrical vortices are limited to the region for $0.75 \leqslant s \leqslant 2$. For sufficiently large initial oscillating displacement of the cylinder, the unstable limit cycle oscillation for $1 \leqslant s \leqslant 1.25$ and $3 < \mathrm{Vr} < 4$ occurs because of

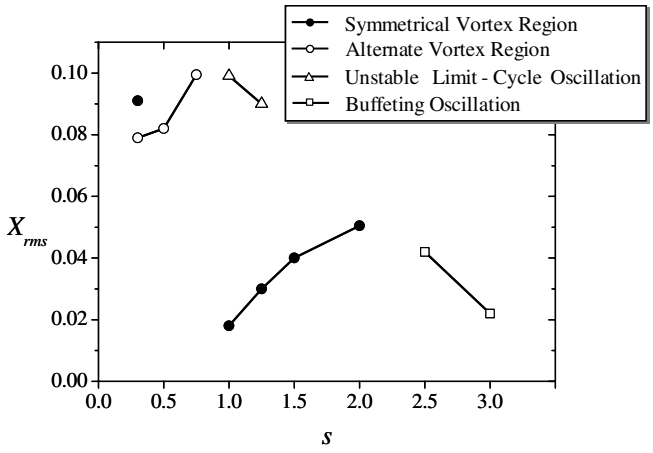

Fig. 12b. The maximum response amplitude of the downstream cylinder in terms of s for $Cn = 0.95$.

alternate Karman vortex shedding from the two cylinders. When s is greater than 2.5, the downstream cylinder experiences buffeting, as results of wake turbulence and velocity fluctuations caused by the upstream cylinder. Fig. 12b shows the maximum response amplitude in the excitation region as a function of s. When s is less than 1, the alternate Karman vortex shedding induces this excitation, of which the maximum amplitudes are twice those for a single cylinder. By increasing s from 1 to 2, the amplitude of oscillation due to the movement-induced excitation gradually increases from 0.02 for $s = 1$ to 0.05 for $s = 2$, while the amplitude due to the buffeting for $2.5 \leqslant s \leqslant 3$, is not so large.

6. Conclusions

Flow-induced streamwise oscillation of two tandem circular cylinders was experimentally studied by free-oscillation testing in a wind tunnel for small values of the reduced mass-damping parameter ($Cn \leqslant 1$). One of the cylinders was elastically supported, so that it could move easily in the streamwise direction, whereas the other was fixed. The distance between them was varied from 0.3 to 3 diameter lengths. The response amplitudes of the oscillating cylinder in streamwise oscillation and the vortex shedding frequency in the wake were measured, and the flow around the cylinders was visualized by the smoke-wire method. The main conclusions of this study are as follows:

(1) The response characteristics when the upstream cylinder is free to oscillate have a wide excitation region in the reduced velocity ($1.4 \leqslant Vr \leqslant 2.5$) and the cylinder gap distance to diameter ratio ($0.3 \leqslant s \leqslant 3$). This consists of movement-induced excitation accompanied by symmetrical vortex shedding from the upstream cylinder, and is promoted by the effect of the downstream cylinder, which acts like a splitter plate.

(2) The other excitation region of the upstream cylinder, which occurs for $2.7 \leqslant Vr \leqslant 3.7$ and is due to alternate Karman vortex shedding, appears for values of s over 1.75 and resembles the streamwise oscillation of a single cylinder, since the influence of the downstream cylinder becomes small.

(3) When the downstream cylinder is free to oscillate, excitation occurs for $2 \leqslant Vr \leqslant 4$ and $0.3 \leqslant s \leqslant 0.75$. The excitation is apparently induced by alternate Karman vortex shedding from the two cylinders, connected by the dead water region between them.

(4) For the range $1 \leqslant s \leqslant 1.25$, the initial oscillating displacement of the downstream cylinder promotes the periodic reattachment of the separated shear layers of the upstream cylinder to the downstream one, which results in an unstable limit-cycle oscillation with large amplitude.

(5) The other excitation regions attributable to symmetrical vortices are limited to the range $0.75 \leqslant s \leqslant 2$. Furthermore, when s is greater than 2.5, the downstream cylinder experiences buffeting, as a result of wake turbulence induced by the upstream cylinder.

Acknowledgements

The authors wish to express their gratitude to Dr. M. M. Zdravkovich and Dr. M. Vynnycky for their helpful comments on the manuscript. This work has been partially supported by the Grants-in-Aid for Scientific Research program of the Japan Society for the Promotion of Science.

References

Assi, G.R.S., Meneghini, J.R., Aranha, J.A.P., Bearman, P.W., Casaprima, E., 2006. Experimental investigation of flow-induced vibration interference between two circular cylinders. Journal of Fluids and Structures 22, 819–827.

Bearman, P.W., 1967. On the vortex street wakes. Journal of Fluid Mechanics 28, 625–641.

Feenstra, P., Weaver, D.S., Nakamura, T.J., 2003. Vortex shedding and fluidelastic instability in a normal square tube array excited by two-phase cross-flow. Journal of Fluids and Structures 17, 793–811.

Ishigai, S., Nishikawa, E., Nishimura, K., Cho, K., 1972. Experimental study on structure of gas flow in tube banks with tube axes normal to flow. Bulletin of the Japan Society of Mechanical Engineers 15, 949–956.

JSME, 2001. JSME Standard S012-1998 Guideline for evaluation of flow-induced vibration of a cylindrical structure in a pipe. JSME International Journal B 44 (4), 682–687.

King, R., Prosser, M.J., Johns, D.J., 1973. On vortex excitation of model piles in water. Journal of Sound and Vibration 29 (2), 169–188.

Laneville, A., Brika, D., 1999. The fluid and mechanical coupling between two circular cylinders in tandem arrangement. Journal of Fluids and Structures 13, 967–986.

Nakamura, A., Okajima, A., 2001. A numerical simulation and vortex structures of in-line oscillation of an elastically supported circular cylinder. In: Proceedings of ASME-PVP Flow-Induced Vibration Symposium, Atlanta, Georgia.

Naudasher, E., Wang, Y., 1993. Flow-induced vibrations of prismatic bodies and grids of prisms. Journal of Fluids and Structures 7, 341–373.

Okajima, A., 1979. Flow around two tandem circular cylinders at very high Reynolds numbers. Bulletin of the Japan Society of Mechanical Engineers 22, 504–511.

Okajima, A., 1982. Aeroelastical oscillation of two tandem circular cylinders. Transactions of RIAM, Kyushu University 57, 247–263, in Japanese.

Okajima, A., Yasuda, T., Iwasaki, T., 2000. Flow visualizations of in-line oscillation of a cylinder with a circular or rectangular section. In: Proceedings of Sixth Triennial International Symposium on FLCOME, FL-048.

Okajima, A., Morishita, M., Nishihara, T., Nakamura, A., 2004a. JSME guideline for evaluation of FIV of a cylindrical structure in a pipe and related researches. In: The 6th International Conference on Nuclear Thermal Hydraulics, Operations and Safety (NUTHOS-6) Nara, N6P160.

Okajima, A., Nakamura, A., Kosugi, T., Uchida, H., Tamaki, R., 2004b. Flow-induced in-line oscillation of a circular cylinder. European Journal of Mechanics B 23, 115–125.

Scruton, C., 1963. On the wind excited oscillations of stacks, towers, and masts. In: Proceedings of International Conference on Wind Effects on Buildings and Structures (Teddington), Her Majesty's Stationery Office.

Tamura, T., Okada, R., 1998. Three-dimensional simulation of bi-directional vortex induced oscillations of a circular cylinder. In: Proceedings of ASME Fluids Engineering Division Meeting, Washington DC, FEDSM 98-5191.